Drastic shrinking of the Hadley circulation during the mid-Cretaceous Supergreenhouse

H. Hasegawa, R. Tada, X. Jiang, Y. Suganuma, S. Imsamut, C. Punya, N. Ichinnorov, Y. Khand

Supplementary Material

Table S1: Paleontological age constraints of the Cretaceous terrestrial deposits in the Asian interior basins

Table S2: Stratigraphic compilation of the climate-sensitive sediments with special emphasis on desert (eolian dune) deposits cited in **Figure 3**.

Supplementary Methods: Paleoposition and Age constraints for the eolian sandstone formations in the Asian interior basins

Figure S1: Lithostratigraphic column, paleowind direction data, and magnetic polarity sequence of the eolian sandstone deposits (Jiaguan Formation) in Sichuan Basin, south China

Figure S2: Lithostratigraphic column, paleowind direction data, and magnetic polarity sequence of the eolian sandstone deposits (Phu Thok Formation) in the Khorat Basin, northeast Thailand

Supplementary References

Table S1: Paleontological age constraints of the Cretaceous terrestrial deposits in the Asian interior basins based on the fossil assemblages of ostracods, charophytes, pollen and spores (modified after, Li, 1982; Racey et al., 1996; Hao et al., 2000; Khand et al., 2000; Meesok, 2000; Chen et al., 2006; Sha, 2007; Hasegawa et al., 2010).

Gobi Basin

Formation	Lithology	Fossil assemblage	Age
Tsagantsav Fm	Reddish brown to whitish grey, conglomerate and sandstone, reddish brown mudstone, calcretes, basalts	Ostracodes: *Cypridea unicostata* Plants: *Baiera manchurica, Cladophiledis onychiopsis, Nilssoniopteris denticulata*	Ber.–Brm.
Shinehudag Fm	Greenish grey to whitish grey, siltstone and mudstone	Ostracodes: *Cypridea fasciculata* Charophytes: *Aclistochara caii, Raskyella sp.* Pollen and Spores: *Cicatricosisporites australiensis, Densoisporites velatus, Pilosisporites trichopapilosus*	Brm?–Apt.
Khukhteeg Fm	Whitish grey to brown, conglomerate, sandstone, mudstone, and lignites	Ostracodes: *Cypridea acutituberculata, Tsetsenia mira, Trapeoidella khandae, Janinella tsaganensis* Charophytes: *Atopochara trivolvis, Mesochara voluta, M. tuzsoni* Pollen and Spores: *Foraminisporites assemmetricus, Alisporites elongatus, Abiespollenites sp.*	Alb.
Bayanshiree Fm	Reddish brown to whitish grey, conglomerate, sandstone, mudstone, and calcretes	Ostracodes: *Lycopterocypris baishintsavica,* Charophytes: *Atopochara multivolvis, Caucasuella gulistanica*	Cen.-San.
Djadokhta Fm	Reddish to reddish brown, eolian sandstone and mudstone	Ostracodes: *Gobiocypris tugrigensis*	e. Camp.
Barungoyot Fm	Reddish to reddish brown, eolian sandstone and mudstone	Ostracodes: *Talicypridea abdarantica*	l. Camp.
Nemegt Fm	Reddish brown to whitish grey, conglomerate, sandstone, mudstone, and calcretes	Ostracodes: *Talicypridea reticulata, Mongolocypris distributa* Charophytes: *Mongololiachara mesochara*	e. Maas.
Dzunmod Fm	Reddish brown to whitish grey, eolian sandstone, mudstone, and calcretes	no fossils	m. Maas.

Ordos Basin

Formation	Lithology	Fossil assemblage	Age
Luohe Fm	Red to purple, fine- to medium-grained, eolian sandstone	Ostracodes: *Darwinula contracta* Vertebrates: *Lycoptera sp.*	Ber.–Vlg.
Huanhe Fm (Huachi Fm)	Yellowish-green to reddish-purple, fine-grained sandstone, siltstone, and mudstone	Ostracodes: *Cypridea unicostata, C. koskulensis, Rhinocypris cirrita* Dinosaurs: *Psittacosaurus sp.*	Vlg.
Luohangdong Fm	Red to purple, fine- to medium-grained, eolian sandstone	Ostracodes: *Cypridea vitimensis, C. consulta, C. koskulensis, Clinocypris scolia, Rhinocypris cirrita, Lycopterocypris infantilis, Darwinula simplus, Rhinocypris foveata, Djungarica stolida* Dinosaurs: *Psittacosaurus youngi*	Vlg.–Hau.
Jingchuang Fm	Yellowish-green to reddish-purple, fine-grained sandstone, siltstone, and mudstone	Ostracodes: *Cypridea unicostata, C. yumenensis, C. justa, C. koskulensis C. consulta, C. subrostrata, Pseudocypridina globra, Clinocypris scolia, Lycopterocypris infantilis, Jungarica stolida, Rhinocypris*	Hau.–Brm.

		foveata, R. cirrita Pollen and Spores: *Cicatricosis porites, Densois porites, Piceae pollenites* Dinosaurs: *Psittacosaurus youngi*	
Lamawan Fm	Yellowish-grey to whitish-grey, medium- to coarce-grained sandstone, mudstone, and coals	Plants: *Elatocladus manchuricus, E. obtusifolia, Brachyphyllum japonicum, Sphenolepidium sp., Coniopteris onychioides, Czekanowskia rigida, Podozamites lanoeolatus, Stenorachis bulunensis*	Brm.–Apt.
Tegaimiao Fm	Red to orange, fine- to medium-grained, eolian sandstone	Dinosaurs: *Protoceratops sp.*	San.–Camp.

Tarim Basin

Formation	**Lithology**	**Fossil assemblage**	**Age**
Kezilesu Gp	Red to purple, conglomerate, sandstone, and sandy mudstone	Ostracodes: *Darwinnela contracta, Cypridea koskulensis, Lycopterocypris circulata, Rhinocypris cirrita,* Charophytes: *Cicatricosisporites sp., Crybelospprites sp.* Pollen and Spores: *Cicatricosis porites, Schizaeois certus, Dicheiropollis etrusus, Crybelospprites sp., Clavatipollenites sp., Liliacidites sp.*	Ber.–Brm.
Kumutake Fm	Red to orange, pebbly sandstone, sandstone, and mudstone	Ostracodes: *Talicypridea meliora, T. gemma, Cypridea cavernosa, C. rostrata, Ziziphocypris simakovi, Candoniella mordvilkoi*	Con.-Camp.
Subashi Fm	Whitish-grey to reddish, medium to coarse-grained sandstone, and mudstone	Ostracodes: *Cypridea mosuowanensi, Talicypridea amoena, T. gemma, T. retusa* Dinosaurs: *Tarbosaurus sp., Nemegtosaurus pachi, Oolithes spherides, Mongolimys turfanensis, Shanshanosaurus huoyanshanensis*	Camp.–Maas.

Subei Basin

Formation	**Lithology**	**Fossil assemblage**	**Age**
Xihengshan Fm	Yellowish grey to purpe, sandstone, mudstone, and coals	Ostracodes: *Cypridea sp.* Plants: *Gleichenites nipponensis, Brachyphyllum besum, Sphenopteris nitidula*	Ber.–Vlg.
Longwangshan Fm	Whitish grey to purple, andesite lava, and andesitic tuff breccia	no fossils	Vlg.
Dawangshan Fm	Purple to grey, andesitic tuff breccia	Plants: *Pagiophyllum sp., Potozamites sp., Otozamites sp.*	Hau.–Brm.
Gecun Fm	Reddish orange, greenish grey, sandstone, and mudstone	Charophytes: *Sphaerochara vertieillata, S. stontoni, Charites symmetrica, Flabellochara jurongica* Pollen and Spores: *Classopollis sp., Cicatricosisporites sp.* Plants: *Frenelopsis sp.*	Apt.-Alb.
Pukou Fm	Reddish-purple to grey, pebbly sandstone	Ostracodes: *Cypridea sp., Talicypridea sp., Ziphocypris simakovi* Pollen and Spores: *Hizaeois porites, Welwitshia pites*	Cen.-Con.
Chishan Fm	Reddish-purple to greenish-grey, sandstone and mudstone	Ostracodes: *Cypridea cavernosa, Talicypridea sp., Eucypris sp.* Plants: *Manica tholistoma*	San.-Maas.

Jianghan Basin

Formation	**Lithology**	**Fossil assemblage**	**Age**
Wulong Fm	Reddish to yellowish-grey,	Ostracodes: *Cypridea prognata, Mantelliana gigantea,*	Alb.

	conglomerate, sandstone, mudstone	*Ziziphocypris simakovi*, *Monosulcocypris sp.* Charophytes: *Mesochara symmetrica, M., stantoni, Flabellochara hangzhouensis, Euaclistochara mundula* Pollen and Spores: *Cicatricosisporites apicanalis, C. tersus, C. dorogensis, C. minutaetritatus, Klukisporites variegatus, Toroisporis pseudodorogensis, Lygodiumsporites subsimplex, Schizaeois porites cretaceousm S. phaseolus* Plants: *Manica parceramosa*	
Luojinghu Fm	Reddish-purple to grey, conglomerate, sandstone	Ostracodes: *Cypridea cavernosa*	Cen.–Tur.
Honghuatao Fm	Reddish to yellowish orange, fine-grained eolian sandstone	Ostracodes: *Cypridea cavernosa, Talicypridea amoena, T. longa* Charophytes: *Porochara anluensis*	Con.–San.
Paomagang Fm	Reddish to whitish grey, sandstone and mudstone	Ostracodes: *Cypridea cavernosa, C. nanxiongensis, C. tera, Talicypridea amoena, T. longa, T. chinensis, T. quadrata* Charophytes: *Latochara cylindrica, L. curtula, L. yunnanensis, Peckichara dangyangensis, Charites tenuis*	Camp.–Maas.

Sichuan Basin

Formation	**Lithology**	**Fossil assemblage**	**Age**
Tianmashan Fm	Reddish-purple conglomerate, sandstone, and mudstone	Ostracodes: *Deyangia lushanensis, D. postacuta, Cypridea sp., Jingguella obtusura, Lycopterocypris sp., Minheella sp., Ziziphocypris sp., Mongolianella sp.*	Ber.–Brm.
Jiaguan Fm	Reddish-purple, fine- to medium-grained, eolian sandstone	Ostracodes: *Cypridea angusticaudata, C. sichuanensis, C. yunnanensis, C. gunzulingensis, C. enodata, C. cf. ampullaceousa, C. concise, C. tera, C. cf. gibbosa, C. setina frorida, C. sentina acerata, C. setina bellatula, C. (Bisulcocypridea) sp., C. (B.) chuxiongensis, C. (Morinina) monosulcata, Harbinia jingshanensin, Latonia (Monosulcocypris) spp., Sinocypris (Quadracypris) cf. favosa, Talicypridea (Cristocypridea) sp., Ziziphocypris orbita, Z. acuta, Jinggunella sp., Kaitunia cuneata,Darwinnela sp., Timiriasevia sp., Lycopterocypris sp., Pinnocypridea sp.*	Apt.–Tur.
Guankou Fm	Red to purple, fine-grained sandstone, mudstone, gypsum	Ostracodes: *Cypridea gigantea, C. infidelis, Cristocypridea latiovata, C. chinensis, Sinocypris subfuningensis, Candona huangdianensis, C. qionglaiensis, Nonion sichuanensis,*	Con.–Maas.

Simao Basin

Formation	**Lithology**	**Fossil assemblage**	**Age**
Jingxing Fm	Yellowish-grey to whitish-grey, sandstone, mudstone, and coals	Ostracodes: *Monosulcocypris reticulata, Cypridea angusticaudata, Candona yunnanensis, Rhinocypris tuberculata, Limnocythere tumulosa*	Ber.–Brm.
Nanxin Fm	Red to purple, sandstone, and mudstone	Ostracodes: *Monosulcocypris subovata, M. subelliptica, M. longa, M. gigantea, M. yunnanensis, M. ventriconvexa, M. reticulata, Ziziphocypris simakovi, Rhinocypris tuberculata* Charophytes: *Atopochara trivolvis, Nodoclavator puchanghensis*	Apt.–Alb.
Bashahe Fm	Reddish-purple, eolian sandstone and sandy mudstone	no fossils	Cen.–Tur.
Mankuanhe Fm	Red to purple, sandy mudstone, and mudstone	Ostracodes: *Eucypris anluensis, Cypridea zhengdongensis, C. cavernosa, Sinocypris*	Con.–Maas.

		zhengdongensis, S. reniformis,Talicypridea subparallela, T. xishuangbananensis, T. amoena Charophytes: *Peckichara dongyangensis, Charites tenuisa*	

Khorat Basin

Formation	Lithology	Fossil assemblage	Age
Phu Kradong Fm	Reddish brown, sandstone, siltstone, and mudstone	Pollen and Spores: *Cyathidites minor, Baculati-sporites commaumensis, Corollina simplex*	E. Cretaceous
Phra Wihan Fm	Whitish-grey, conglomerate, sandstone, mudstone, and lignites	Pollen and Spores: *Cicatricosisporites augustus, Dicheiropollis etruscus, Corollina spp., Araucariacites australis, Ischyosporites cf. variegatus, Gleichenidites senonicus, Laevigatosporites sp., Perinopollenites elatoides, Callialasporites dampieri, Anaplanisporites dawsonensis, Apiculatisporites spp., Osmundacidites wellmanii, Todisporites minor, Kraeuselisporites sp., Concavissmisporites sp.*	Ber.–Brm.
Sao Khua Fm	Reddish brown, sandstone, siltstone, and mudstone	Pollen and Spores: *Vitreisporites cf. pallidus, Cicatricosisporites spp., Cyathidites minor spp., Ephedripites spp., ?Araucariacites australis*	E. Cretaceous
Phu Phan Fm	Whitish-grey, conglomerate, sandstone, mudstone	Pollen and Spores: *Corollina spp., Cyathidites minor, ?Todisporites sp.*	E. Cretaceous
Khok Kruat Fm	Reddish brown, sandstone, siltstone, and mudstone	Pollen and Spores: no data presented*	Apt.?
Maha Sarakhan Fm	Reddish, sandstone, siltstone, salts, gypsums, and anhydrites	Pollen and Spores: no data presented*	Alb.?–Cen.?
Phu Thok Fm	Reddish, eolian sandstone and siltstone	no fossils	Apt.–Tur.?
Phu Khat Fm	Reddish to whitish grey, sandstone and mudstone	no fossils	L. Cretaceous

*Palynological age estimatioins of the Khok Kruat and Maha Sarakham Formations are quoted by Sattayarak et al. (1991a,b). However, no palyno-fossil assemblage data were presented.

Table S2: Stratigraphic compilation of the climate-sensitive sediments with special emphasis on desert (eolian dune) deposits cited in **Figure 3**.

Locality No.	Basin	Formation	Lithology	Age	References
1	Gobi basin, Mongolia	Khukhteeg and Bayanshiree Fms	Whitish-grey, conglomerate, sandstone, mudstone, lignite, and Reddish-brown to whitish-grey, conglomerate, sandstone, mudstone	Alb. to Cen.–San.	Jerzykiewicz and Russell, 1991; Khand et al., 2000
2	Subei basin, China	Gecun and Pukou Fms	Reddish-orange to greenish-grey, sandstone, mudstone, and Reddish-purple to grey, pebbly sandstone	Apt.-Alb. to Cen.-Con.	Jiang and Li, 1996; Hao et al., 2000
3	Jianghan basin, China	Wulong and Luojinghu Fms	Reddish to yellowish-grey, conglomerate, sandstone, mudstone and Reddish-purple to grey, conglomerate, sandstone	Alb. to Cen.–Tur.	Jiang and Li, 1996; Hao et al., 2000
4	Sichuan basin, China	Jiaguan Fm	Reddish-purple, fine- to medium-grained, eolian sandstone	Apt.–Tur.	Jiang et al., 2001
5	Simao basin, China	Nanxin and Bashahe Fms	Reddish-purple, sandstone, mudstone and Reddish-purple, eolian sandstone, sandy mudstone	Apt.–Alb. to Cen.–Tur.	Jiang et al., 2001
6	Khorat basin, Thailand	Maha Sarakhan and Phu Thok Fms	Reddish, sandstone, siltstone, salts, gypsums, and Reddish, eolian sandstone, siltstone	Apt.–Tur.?	Imsamut, 1996; Hasegawa et al., 2010
7	Iberian basin, Spain	Escucha and Utrillas Fms	Fine-grained eolian sandstone, siltstone, mudstone	Alb.–Cen.	Rodriguez-Lopez et al., 2006, 2008
8	British Columbia, Canada	Boulder Creek Fm	Grayish very fine-grained sandstone, Greenish-gray mudstone, sphaerosiderite- bearing paleosol	Alb.–Cen.	Leckie et al., 1989; Ufnar et al., 2005
9	North Alberta, Canada	Peace River Fm	Grayish sandstone, mudstone, sphaerosiderite-bearing paleosol	Alb.–Cen.	Ufnar et al., 2005
10	South Alberta, Canada	Mill Creek and Bow Island Fms	Reddish and grayish-greenish sandstone, pale yellow to dark red mudstone, paleosol	Alb.	McCarthy et al., 1997, 1999
11	Ontario basin, Canada	Mattagami Fm	Varicolored conglomerate, sandstone, mudstone, lignite	Apt.–Alb. to Cen.	White et al., 2000
12	Western Iowa basin	Dakota and Swan River Fms	Grayish sandstone, mudstone, sphaerosiderite-bearing paleosol	Alb.–Cen.	Ludvigson et al., 1998; White et al., 2000
13	Southwest Utah basin	Upper part of the Dakota Fm	Varicolored conglomerate, sandstone, mudstone, coal	Cen.–Tur.	Laurin and Sageman, 2007; Barclay et al., 2010
14	New Mexico basin	Sarten and Moreno Hill Fms	Reddish to pale yellowish sandstone, mudstone, paleosol	Alb.–Cen. to Tur.	Mack, 1992
15	Araripe basin, Brazil	Santana Fm	Sandstone, mudstone, black shale	Alb.	Heimhofer et al., 2008
16	Salta basin, Algentina	La Yesera Fm	Reddish-brown conglomerate, sandstone, siltstone, mudstone	Apt.–Alb.	Marquillas et al., 2005
17	Neuquen basin, Algentina	Lohan Cura Fm	Reddish-brown to greenish gray conglomerate, sandstone, siltstone,	Apt.–Alb.	Leanza et al., 2004

			shale		
18	Orange basin, Namibia	Alb. to Cen. succession	Whitish conglomerate, sandstone, siltstone, mudstone	Alb.–Cen.	Stevenson and McMillan, 2004;
19	Tendaguru basin, Tanzania	Makonde Fm	Reddish to purple, conglomerate, fine- to medium-grained sandstone, siltstone, mudstone	Apt.–Alb.	Bussert et al., 2009
20	Saurashtra basin, India	Than and Wadhwan Fms	Grayish sandstone, mudstone, coal and Reddish conglomerate, sandstone, mudstone, limestone	E. Cretaceous	Aslam, 1992
21	Gippsland basin, Australia	Wonthaggi Fm	Volcanogenic sandstone, mudstone, coal	Apt.–Alb.	Douglas and Williams, 1982; Tosolini et al., 2002
22	Gobi basin, Mongolia	Djadokhta, Barungoyot, Dzunmod Fms	Reddish brown to whitish grey, eolian sandstone, sandy mudstone, calcrete	Camp.–Maas.	Jerzykiewicz and Russell, 1991; Hasegawa et al., in submitted
23	Ordos basin, China	Tagaimiao Fm	Red to orange, fine- to medium-grained, eolian sandstone	San.–Camp.	Jiang and Li, 1996; Hao et al., 2000
24	Tarim basin, China	Subashi Fm	Whitish-grey to reddish, medium to coarse-grained sandstone, mudstone	Camp.–Maas.	Jiang and Li, 1996; Hao et al., 2000
25	Subei basin, China	Chishan Fm	Reddish-purple to greenish-grey, sandstone, mudstone	San.-Maas.	Jiang and Li, 1996; Hao et al., 2000
26	Jianghan basin, China	Paomagang Fm	Reddish to whitish grey, sandstone, mudstone	Camp.–Maas.	Jiang and Li, 1996; Hao et al., 2000
27	Sichuan basin, China	Guankou Fm	Red to purple, fine-grained sandstone, mudstone, gypsum	Con.–Maas.	Jiang et al., 2001
28	Simao basin, China	Mankuanhe Fm	Red to purple, sandy mudstone, mudstone	Con.–Maas.	Jiang et al., 2001
29	Khorat basin, Thailand	Phu Khat Fm	Reddish to whitish grey, sandstone, mudstone	L. Cretaceous	Hasegawa et al., 2010
30	South Alberta, Canada	Belly River and Willow Creek Fms	Reddish brown to whitish grey, conglomerate, sandstone, mudstone, calcrete	Camp.–Maas.	Jerzykiewicz and Sweet, 1988;
31	Western Montana basin, Canada	Two Medicine Fm	Reddish brown to whitish grey, conglomerate, sandstone, mudstone, calcrete	Camp.–Maas.	Lorenz, 1981
32	Eastern Montana basin, Canada	Hell Creek Fm	Varicolored conglomerate, sandstone, mudstone, coal	Maas.	Retallack, 1994; Johnson et al., 2002
33	North Dakota basin	Hell Creek Fm	Varicolored conglomerate, sandstone, mudstone, coal	Maas.	Fastovsky and McSweeney, 1987 Johnson et al., 2002
34	Southwest Utah basin	Wahweap and Kaiparowits Fms	Varicolored conglomerate, sandstone, mudstone	Camp.–Maas.	Lawton et al., 2003
35	New Mexico basin	MacRae Fm	Reddish-brown to greyish, conglomerate, sandstone, mudstone, calcrete	Maas.	Buck and Mack, 1995
36	Western Texas basin	Aguja and Javelina Fms	Reddish purple to grayish, sandstone, mudstone, paleosol	Maas.	Lehman, 1989, 1990
37	Salta basin,	Lecho Fm	Whitish, fine- to medium-grained,	Maas.	Marquillas et al., 2005

	Algentina		eolian sandstone		
38	Bauru basin, Brazil	Rio Parana Fm, Caiua Gp.	Fine- to medium-grained, quartz eolian sandstone	Con.–Maas.	Fernandes et al., 2007
39	Parana basin, Brazil	Marilia Fm	Medium- to coarse-grained, quartz-feldspar eolian sandstone, calcretes	Maas.	Goldberg and Garcia, 2000
40	Neuquen basin, Algentina	Anacleto and Allen Fms	Reddish to greenish-gray, conglomerate, sandstone, siltstone, mudstone	San.–Maas.	Leanza et al., 2004
41	Anambra basin, Namibia	Mamu and Ajali Fms	Conglomerate, sandstone, shale, coal	Camp.–Maas.	Tuttle, 1999
42	Congo basin, Angola	Nsele Gp	Medium- to coarse-grained sandstone, eolian accumulation texture	L.Cretaceous	Giresse, 2005
43	Orange basin, Namibia	Upper Santonian succession	Brownish sandstone, mudstone	L. Santonian	Stevenson and McMillan, 2004;
44	Dongargaonba sin, India	Lameta Fm	Reddish to greenish, conglomerate, sandstone, mudstone, calcrete	Maas.	Mohabey et al., 1993; Mohabey, 1996
45	Gippsland basin, Australia	Latrobe Gp.	Conglomerate, sandstone, mudstone, coal, volcanics	Camp.–Maas.	Wagstaff et el., 2006; Gallagher et al., 2008

Supplementary Methods:

Paleoposition of eolian sandstone deposits in Asian interior basins

Paleolatitude and rotation estimates of the studied basins, which are reconstructed based on paleomagnetic data (Cheng et al., 1988; Zhuang, 1988; Otofuji et al., 1990; Enkin et al., 1991; Zheng et al., 1991; Chen et al., 1993; Huang and Opdyke, 1993; Hankard et al., 2005; Charusiri et al., 2006; **Fig. 1** and **Table 1**), are the critical basis for the present study which demonstrate that the location of the subtropical high-pressure belt changed significantly during the Cretaceous. Based on the obtained paleomagnetic data sets, paleolatitudes of the North China block (Ordos Basin: N32.6˚–41.0˚; Cheng et al., 1988; Zheng et al., 1991) and the South China block (Sichuan Basin: N25.5˚–29.6˚; Zhuang *et al.*, 1988; Enkin et al., 1991) were different by more than 5˚ during the Cretaceous (**Fig. 1** and **Table 1**). The Gobi Basin of southern Mongolia was located much higher latitude during the Cretaceous (N44.0˚–46.1˚; Hankard et al., 2005). Reconstruction of the paleoposition of Indochina block during the Cretaceous, prior to the India-Asia collision, has been controversial. For example, Chen *et al*. (1992) argued that both Indochina block and South China block were located between N20˚ and N30˚ during the Cretaceous, based on the paleomagnetic data reported by Yang and Basse (1993). However, the paleomagnetic data reported by Yang and Basse (1993) is for the upper Triassic to the lower Cretaceous deposits in the Khorat Basin (Indochina block) in northeastern Thailand, and no paleomagnetic data of the mid- to upper Cretaceous deposits, which contain eolian sandstone deposits in this area, was reported. On the other hand, Charusiri et al. (2006) conducted the paleomagnetic study on the mid- to upper Cretaceous deposits in the Khorat Basin, northeastern Thailand for the first time. They concluded that the Khorat Basin was located between N16.3˚ and 21.6˚ during the mid- to late Cretaceous time (Charusiri et al., 2006), which was much lower than that of South China block (N25.5˚–29.6˚; Zhuang *et al.*, 1988; Enkin et al., 1991). Therefore, eolian sandstones were distributed in ca. N30˚–40˚ (Ordos and Tarim basins) during the early Cretaceous, shifted southwards to ca. N20˚–30˚ (Sichuan and Khorat basins) during the mid-Cretaceous, and shifted northwards again to ca. N30˚–45˚ (Gobi and Ordos basins) during the late Cretaceous, implying that the significant latitudinal shifts of the distribution of eolian sandstone deposits have occurred between the early, mid-, and late Cretaceous (**Fig. 1**).

Age constraints for eolian sandstone formations in Asian interior basins

Although non-marine strata generally have chronostratigraphic uncertainties, our selected data sets of eolian sandstone formations in the Asian interior basins have good age controls based on magnetostratigraphy and/or biostratigraphy (Li, 1982; Jerzykiewicz and Russell, 1991; Jiang and Li, 1996; Racey et al., 1996; Hao et al., 2000; Khand et al., 2000; Meesok, 2000; Jiang et al., 2001; Chen et al., 2006; Sha, 2007; **Fig. 1** and **Table S1**), including the results of our magnetostratigraphic studies (Imsamut, 1996; Pan et al., 2004; Hasegawa et al., 2010; **Figs. S1, S2**). Paleontological age constraints provide a starting point for the ages of the eolian sandstone formations cited in this study. A relatively rich record of fossil ostracods, charophytes, plants, pollens, and spores has been collected from the studied sites (**Table S1**). Particularly important are the ages of the eolian sandstone formations in Sichuan Basin and Khorat Basin (the Jiaguan Formation and the Phu Thok Formation), because they provide the critical time constraints on the low latitude desert distribution during the mid-Cretaceous. The ages of these formations are well constrained by our magnetostratigraphic data (Imsamut, 1996; Pan et al., 2004; Hasegawa et al., 2010) in conjunction with paleontological age constraints as described below.

The age of the Jiaguan Formation in Sichuan Basin is assigned to the Aptian–Turonian based on the ostracod's biostratigraphy of the Jiaguan Formation, which yields age-diagnostic ostracodes such as *Ziziphocypris orbita*, *Cypridea (Bisulcocypridea)* sp. (Cenomanian–Turonian), and *Latonia (Monosulcocypris)* spp. (Aptian) (Li, 1982; Hao et al., 2000; Chen et al., 2006; **Table S1**). Such age constraint is consistent with the ostracod's biostratigraphy of the underlying Tianmashan Formation (Berriasian–Barremian) and overlying Guankou Formation (Coniacian–Maastrichtian). In addition, the obtained paleomagnetic polarity sequence of the Jiaguan Formation reveals short repetition of reverse-normal-reverse polarity changes in its lowermost part and thick normal polarity zone in its main part (Pan et al., 2004), which correlate best with chron M1r to superchron C34n of the geomagnetic polarity time scale (GPTS; Gradstein et al., 2004). These results suggest that deposition of the Jiaguan Formation began approximately at 127 Ma and ended no later than ca. 84 Ma (from late Barremian–early Aptian to no later than late Santonian) (Pan et al., 2004; **Fig. S1**).

Age constraints of the Phu Thok Formation in Khorat Basin are provided by the palynological evidences of the underlying strata, the lignite-bearing Phra Wihan Formation, which yields

age-diagnostic palyno-fossils such as *Cicatricosisporites augustus* indicating the age no older than Berriasian and *Dicheiropollis etruscus* indicating the age of Barremian (Racey et al., 1996). Thus, age of the Phra Wihan Formation is assigned to the early Cretaceous (Berriasian–Barremian), and the age of the overlying Phu Thok Formation is younger than Barremian age (Racey et al., 1996; Meesok, 2000; DMR, 2001; Charusiri et al., 2006; **Table S1**). Our newly established paleomagnetic polarity sequence of the Phu Thok Formation reveals short repetition of reverse-normal-reverse polarity changes in its lowermost part and thick normal polarity zone in its main part (Imsamut, 1996; Hasegawa et al., 2010; **Fig. S2**), which can be correlated with chron M1n to superchron C34n of the GPTS (Gradstein et al., 2004). Consequently, deposition of the Phu Thok Formation is interpreted as having started approximately at 126 Ma and ended no younger than ca. 84 Ma (from late Barremian–early Aptian to no younger then late Santonian), which is approximately the same age as the Jiaguan Formation in Sichuan Basin. In summary, the low latitude deserts in Asia emerged between late Barremian and early Aptian and disappeared between Turonian and Coniacian according to the magnetostratigraphic correlations and paleontological age constraints of the eolian sandstone formations in the Sichuan Basin (Jiaguan Formation) and the Khorat Basin (Phu Thok Formation) given above (**Fig. 1**).

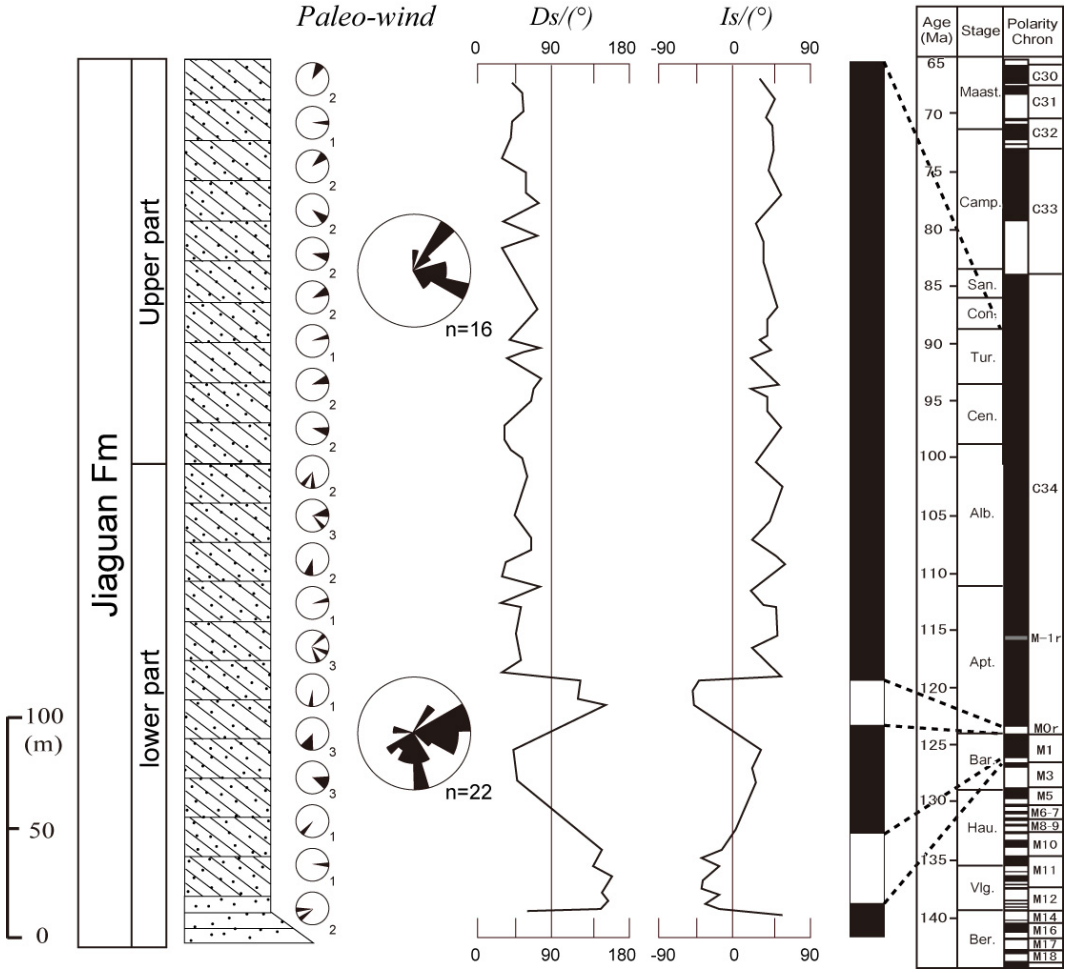

Fig. S1: Lithostratigraphic column, paleowind direction data, and magnetic polarity sequence of the eolian sandstone deposits (Jiaguan Formation) in Sichuan Basin, south China (Jiang et al., 1999; Pan et al., 2004; Hasegawa et al., 2010), and their correlation to the geomagnetic polarity time scale (GPTS) of the geological time scale 2004 (Gradstein et al., 2004). Magnetic polarity zones are shown by black and white bars for normal and reversed polarities.

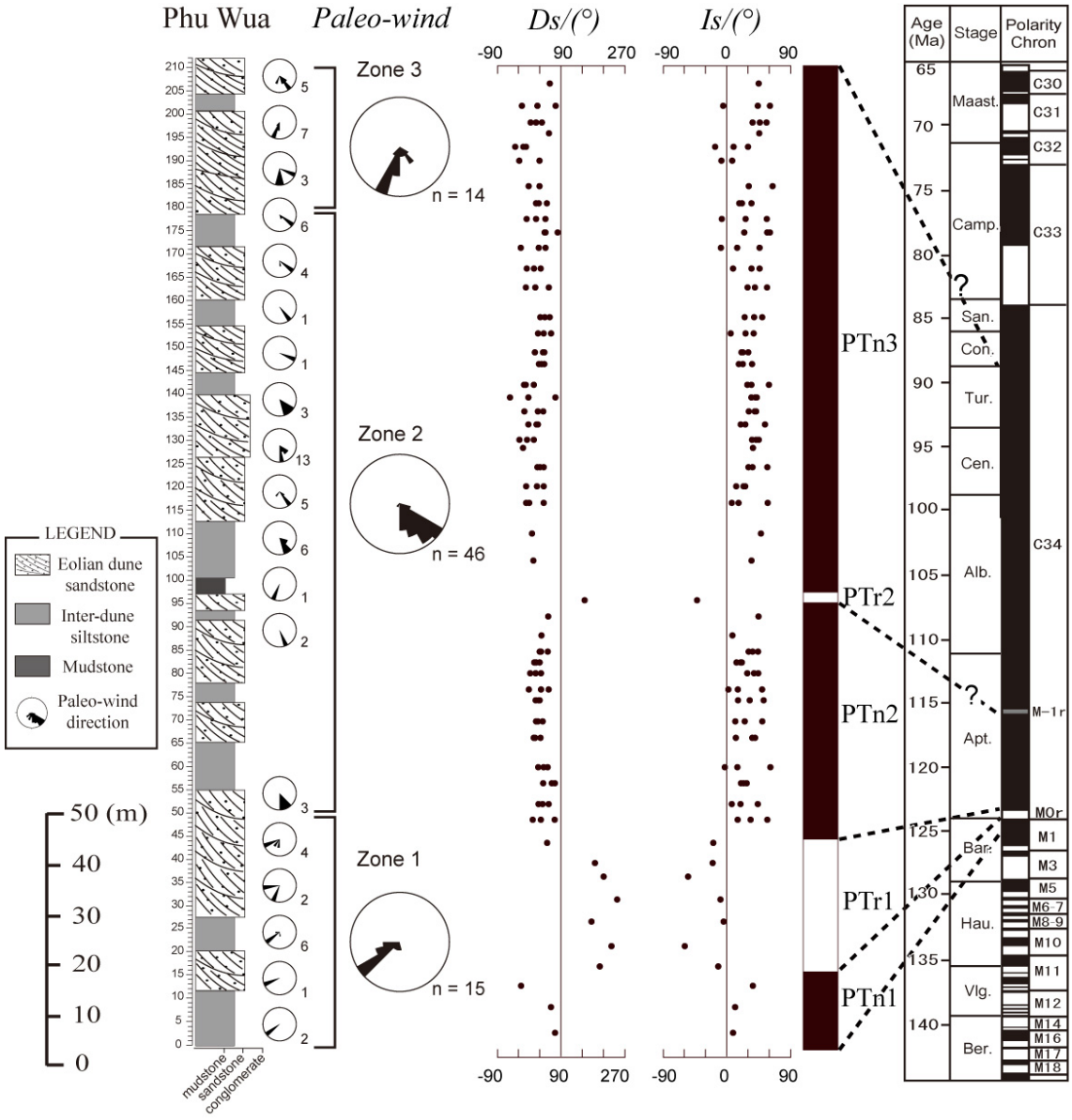

Fig. S2: Lithostratigraphic column, paleowind direction data, and magnetic polarity sequence of the eolian sandstone deposits (Phu Thok Formation) in the Khorat Basin, northeast Thailand (Imsamut, 1996; Hasegawa et al., 2010), and their correlation to the GPTS (Gradstein et al., 2004). Magnetic polarity zones are shown by black (white) bars for normal (reversed) polarity.

Supplementary References

Aslam, M., 1992. Delta plain coal deposits from the Than Formation of the Early Cretaceous Saurashtra basin, Gujarat, western India. Sedimentary Geology 81, 181–193.

Barclay, R.S., McElwain, J.C., Sageman, B.B., 2010. Carbon sequestration activated by a volcanic CO2 pulse during Ocean Anoxic Event 2. Nature Geoscience 3, 205–208.

Buck, B.J., Mack, G.H. 1995. Latest Cretaceous (Maastrichtian) aridity indicated by paleosols in the McRae Formation, south-central New Mexico. Cretaceous Research 16, 559–572.

Bussert, R., Heinrich, W.D., Aberhan, M., 2009. The Tendaguru Formation (Late Jurassic to Early Cretaceous, southern Tanzania): definition, palaeoenvironments, and sequence stratigraphy. Fossil Record 12, 141–174.

Douglas, J.G., Williams, G.E., 1982. Southern polar forests: The Early Cretaceous floras of Victoria and their palaeoclimatic significance. Palaeogeography, Palaeoclimatology, Palaeoecology 39, 171–185.

Fastovsky, D.E., McSweeney, K., 1987. Paleosols spanning the Cretaceous-Paleogene transition, eastern Montana and western North Dakota. Geological Society of America Bulletin 99, 66–77.

Gallagher, S.J., Wagstaff, B.E., Baird, J.G., Wallace, M.W., Li, C.L., 2008. Southern high latitude climate variability in the Late Cretaceous greenhouse world. Global and Planetary Change 60, 351–364.

Hasegawa, H., Suganuma, Y., Seike, K., Tada, R., Ichinnorov, N., Badamgarav, D., Khand, Y., in submitted. Magnetostratigraphy and depositional environments of Upper Cretaceous deposits in the Gobi Basin, southern Mongolia: implications for desert development in mid-latitude Asia. (submitted to *Journal of Asian Earth Sciences*)

Heimhofer, U., Hesselbo, S.P., Pancost, R.D., Martill, D.M., Hochuli, P.A., Guzzo, J.V.P., 2008. Evidence for photic-zone euxinia in the Early Albian Santana Formation (Araripe Basin, NE Brazil). Terra Nova 20, 347–354.

Jerzykiewicz, T., Sweet, A.R., 1988. Sedimentological and palynological evidence of regional climatic changes in the Campanian to Paleocene sediments of the Rocky Mountain Foothills, Canada. Sedimentary Geology 59, 29–76.

Jiang, X.S., Pan, Z.X., Fu, Q.P., 1999. The variations of palaeowind direction of the Cretaceous desert in the Sichuan Basin and their significance. Sedimentary Facies and Palaeogeography 19, 1–11.

Johnson, K.R., Nichols, D.J., Hartman, J.H., 2002. Hell Crek Formation: A 2001 synthesis.

Geological Society of America Special Paper 361, 503–510.

Laurin, J., Sageman, B., 2007. Cenomanian_Turonian coastal record in SW Utah, USA: Orbital scale transgressive-regressive events during Oceanic Anoxic Event II. Journal of Sedimentary Research 77, 731–756.

Lawton, T.F., Polloch, S.L., Robinson, R.A.J., 2003. Integrating sandstone petrology and nonmarine sequence stratigraphy: Application to the late cretaceous fluvial systems of southwestern Utah, USA. Journal of Sedimentary Research 73, 389–406.

Leanza, H.A., Apesteguıia, A., Novas, F.E., de la Fuente, M.S., 2004. Cretaceous terrestrial beds from the Neuque´n Basin (Argentina) and their tetrapod assemblages. Cretaceous Research 25, 61–87.

Leckie, D., Fox, C., Tarnocai, C., 1989. Multiple paleosols of the late Albian Boulder Creek Formation, British Columbia, Canada: Sedimentology 36, 307–323.

Lehman, T.M., 1989. Upper Cretaceous (Maastrichtian) Paleosols in Trans-Pecos Texas. Geological Society of America Bulletin 101, 188–203.

Lehman, T.M., 1990. Paleosols and the Cretaceous/Tertiary transition in the Big Bend region of Texas. Geology 18, 362–364.

Lorenz, J.C., 1981. Sedimentary and tectonic history of the Two Medicine Formation, Late Cretaceous (Campanian), northwestern Montana. Ph.D. Thesis, Princeton University, Princeton, N.J., pp.214 .

Mack, G.H., 1992. Paleosols as an indicator of climatic-change at the early-late Cretaceous boundary, Southwestern New Mexico. Journal of Sedimentary Petrology 62, 483–494.

McCarthy, P.J., Martini, I.P., Leckie, D.A., 1997. Anatomy and evolution of a Lower Cretaceous alluvial plain: Sedimentology and palaeosols in the upper Blairmore Group, south-western Alberta, Canada. Sedimentology 44, 197–220.

McCarthy, P.J., Martini, I.P., Leckie, D.A., 1999. Pedogenic and diagenetic influences on void coating formation in Lower Cretaceous paleosols of the Mill Creek Formation, southwestern Alberta, Canada. Geoderma 87, 209–237.

Mohabey, D.M., Udhoji, S.G., Verma, K.K., 1993. Palaeontological and sedimentological observations on non-marine Lameta Formation (Upper Cretaceous) of Maharashtra, India: their palaeeoecological and palaeoenvironmental significance. Palaeogeography, Palaeoclimatology, Palaeoecology 105, 83–94.

Mohabey, D.M., 1996. A new oospecies, Megaloolithus matleyi, from the Lameta Formation (Upper Cretaceous) of Chandrapur district, Maharashtra, India, and general remarks on the

palaeoenvironment and nesting behaviour of dinosaurs. Cretaceous Research 17, 183–196.

Racey, A., Love, M. ., Canham, A. C., Goodall, J. G. S., Polachan, S., and Jones, P. D.: Stratigraphy and reservoir potential of the Mesozoic Khorat Group, NE Thailand, J. Petrol. Geol., 19, 5–40, 1996.

Retallack, G.J., 1994. A pedotype approach to latest Cretaceous and earliest Tertiary paleosols in eastern Montana. Geological Society of America Bulletin 106, 1377–1397.

Rodriguez-Lopez, J.P., de Boer, P.L., Melendez, N., Soria, A.R., Pardo, G., 2006. Windblown desert sands in coeval shallow marine deposits: a key for the recognition of coastal ergs in the mid-Cretaceous Iberian Basin, Spain. Terra Nova 18, 314–320.

Sattayarak, N., Srigulwong, S., Pataramethа, M., 1991a. Subsurface stratigraphy of the non-marine Mesozoic Khorat Group, Northern Thailand. GEOSEA VII, Bangkok, 36A.

Sattayarak, N., Polachan, S., Charusirisawad, R., 1991b. Cretaceous rock salt in the northeastern part of Thailand. GEOSEA VII, Bangkok, 36A.

Stevenson, I.R., McMillan, I.K., 2004. Incised valley fill stratigraphy of the Upper Cretaceous succession, proximal Orange Basin, Atlantic margin of southern Africa. Journal of the Geological Society, London 161, 185–208.

Tosolini, A.M.P., McLoughlin, S., Drinnan, A.N., 2002. Early Cretaceous megaspore assemblages from southeastern Australia. Cretaceous Research 23, 807–844.

Tuttle, M.L.W., Charpentier, R.R., Brownfield, M.E., 1999. The Niger Delta Petroleum System: Niger Delta Province, Nigeria, Cameroon, and Equatorial Guinea, Africa. Open-File Report, U.S. Department of the Interior, U.S. Geological Survey, pp.64.

Ufnar, D. F., Gonzalez, L. A., Ludvigson, G. A., Brenner, R. L., Witzke, B. J. Leckie, D., 2005. Reconstructing a mid-Cretaceous landscape from paleosols in western Canada. Journal of Sedimentary Research75, 984–996.

Wagstaff, B.E., Gallagher S.J.,Lanigan, K.P., 2006. Late Cretaceous palynological correlation and environmental analysis of fluvial reservoir facies of the Tuna Field, Gippsland Basin, southeast Australia. Review of Palaeobotany and Palynology 138, 165–186.

White, T.S., Witzke, B., Ludvigson, G., 2000. Evidence for an Albian Hudson Arm of the North American Cretaceous Western Interior Seaway. Geological Society of America Bulletin 112, 1342–1355.

Yang, Z., and Basse, J.: Paleomagnetic study of Permian and Mesozoic sedimentary rocks from Northern Thailand supports the exteuction model for Indochina, Earth Planet. Sc. Lett., 117, 525–552, 1993.